

Optimization of Electrospinning an SU-8 Negative Photoresist to Create Patterned Carbon Nanofibers and Nanobeads

Jeremy K. Steach, Jonathan E. Clark, Susan V. Olesik

Department of Chemistry, The Ohio State University, Columbus, Ohio 43210

Received 13 May 2009; accepted 11 October 2009

DOI 10.1002/app.31597

Published online 20 May 2010 in Wiley InterScience (www.interscience.wiley.com).

ABSTRACT: The optimization of electrospinning SU-8 2100 negative photoresist was performed to create carbon micro/nanofibers and beads that can be patterned after electrospinning by using UV radiation. The fiber diameters had a range of 300 nm to 1 μ m, based upon the selected electrospinning parameters. Low concentrations of the SU-8 2100 resulted in beads while specific higher concentrations produced well-defined fibers. Fibers and beads were converted to carbon through pyrolysis and retained

their three dimensional structure. By utilizing the photosensitive properties of the SU-8 negative photoresist, the electrospun fibers were patterned by UV photolithography. The fibers and beads were characterized by SEM and Raman microscopy, respectively. © 2010 Wiley Periodicals, Inc. *J Appl Polym Sci* 118: 405–412, 2010

Key words: nanotechnology; photopolymerization; photoresist; processing

INTRODUCTION

Electrospinning of polymeric fibers provides the capability to create micro/nanofibers through an inexpensive and simple method.¹ Electrospun micro/nanofibers have been applied to many different applications ranging from tissue scaffolds,² sensors,^{3–6} and electronics.^{7,8} Electrospinning involves placing a high electric field between a polymer solution and a conductive collector. When the electric field is strong enough to overcome the surface tension of the droplet, a Taylor cone is formed. Following the creation of the Taylor cone, fibers are ejected toward the conductive collector.⁹ Using this technique, many different polymers and polymer blends can be used to fabricate fibers with various chemical compositions.

Using this technique, several groups have used various polymers to create carbon fibers. Carbon nanofibers were created by pyrolyzing electrospun polyacrylonitrile (PAN),^{10–12} pitch,¹³ polyimide,¹⁴ polymer blends of poly (ϵ -caprolactone), and poly (methyl methacrylate) with and without carbon nanotubes added to the polymer solution.¹⁵ Other common methods to create carbon nanofibers are chemical vapor deposition (CVD)¹⁶ and hydrocarbon pyrolysis,¹⁷ which can generate fibers ranging from

a few microns down to 10 nm or 100–800 nm, respectively.

Although electrospun carbon fibers have been produced, these fibers are typically produced in an unpatterned, nonwoven mat. The advantage of electrospinning SU-8 is that the mat of fibers can be patterned after they are spun by using UV radiation. To date, the electrospinning methods that produced patterned fibers are due to the patterned collectors used.^{18–20} By using different collectors, other groups have forced the fibers into different patterns. These collectors have consisted of wire meshes, metal patterned onto insulating substrates, screws, or patterned metal templates. By using the SU-8 photoresist to electrospin micro/nanofibers, the nonwoven fiber mats can easily be patterned after the fibers are electrospun on a conductive substrate of choice.

SU-8 is an epoxy-based, negative photoresist. Cured polymeric films of SU-8 are highly resistant to solvents, acids, and bases. SU-8 solutions are highly viscous, which makes it ideal for electrospinning; however, its low molecular weight provides solubility in a wide range of organic solvents.²¹ This work takes advantage of SU-8's solubility in cyclopentanone in order to deduce the optimal concentration for electrospinning purposes.

Herein, the electrospinning parameters used to create the SU-8 2100 fibers and nanobeads, the conversion of these fibers to carbon through pyrolysis, and the ability to pattern these fibers with UV radiation after electrospinning are described. The focus of this work was to produce the smallest diameter

Correspondence to: S. V. Olesik (olesik.1@osu.edu).

fibers and beads as possible. Optimal parameters for electrospinning SU-8 2100 photoresist and the characterization of these fibers and beads before and after pyrolysis are also discussed.

EXPERIMENTAL

Materials

All materials were used as received. SU-8 2100 negative photoresist and SU-8 developer was purchased from MicroChem Corp. (Newton, MA). The solvent used to prepare the dilute SU-8 2100 solutions were cyclopentanone (Aldrich). 100% SU-8 2100 was examined, as were dilutions of 75, 70, 50, 25, and 0% (v/v) (SU-8 2100/ cyclopentanone). The solutions were stirred in a sample vial for 2 days to ensure that the final solutions were homogenous. All solutions were drawn into 10 mL syringes and were placed vertically so that all air could be removed before electrospinning.

Electrospinning apparatus

For electrospinning experiments, a Spellman CZE 1000R (Hauppauge, NY) was used to supply voltages from 5 to 15 kV. A Harvard Model 33 dual syringe pump was used to control the flow rate of the SU-8 2100 solutions. The flow rates were varied from 0 to 2 mL/min. Cleaved silicon pieces from a silicon wafer were used as the collector for the fibers. All electrospinning experiments were performed under yellow light to ensure that the SU-8 solutions were not crosslinked. Electrospinning experiments were performed while varying the following parameters: SU-8 2100/cyclopentanone (v/v) concentrations, voltage, flow rate, and distance. From these results, the optimal electrospinning parameters were determined. After each experiment, the fibers were exposed to a UV light to crosslink the SU-8 fibers. All samples were then transferred to clean sample vials, which were capped for storage. Each fiber sample was inspected with an Olympus BX51 optical microscope using 10 \times and 50 \times objectives to determine if fibers or beads were present on the silicon.

Pyrolysis of electrospun SU-8 fibers

Samples were prepared in sets of two by the electrospinning method described earlier. After electrospinning, both samples were exposed to UV radiation for \sim 5 min. One sample was then kept in a vial and the other was placed in the furnace for pyrolysis. This was done so that each sample could be compared before and after pyrolysis. The pyrolyzed samples were placed in a Lindberg/Blue TF55030A

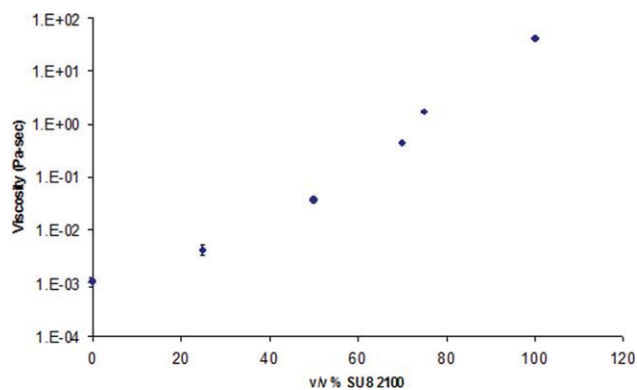


Figure 1 Viscosity measurements for the % (v/v) SU-8 2100 solutions attempted at electrospinning. [Color figure can be viewed in the online issue, which is available at www.interscience.wiley.com.]

quartz tube furnace after being exposed to the UV source for \sim 5 min. The sample was then placed inside the quartz tube. A forming gas mixture (95% N₂ and 5% H₂) was flowed through the quartz tube to remove any oxygen. After flowing the forming gas through the tube for 20 min, the pyrolysis of the fibers was started. The furnace was ramped at 1°C/min to a final temperature of 800°C. Forming gas flowed continuously for the duration of the pyrolysis. The final temperature was held for a minimum of 5 h before the pyrolysis was stopped. After the furnace was turned off, the sample was allowed to cool to room temperature (25°C) under a constant flow of forming gas. Samples were then removed and placed into clean sample vials and capped.

UV photopatterning of electrospun SU-8 fibers

To pattern the fibers, the SU-8 was first electrospun onto the silicon collector as described earlier. The pattern was created by using a lithographic mask or by printing the desired shape onto a transparency. The lithographic mask or transparency was placed onto the fibers and then the fibers were exposed to the UV source (Sunray 400 SM, Uvitron International, West Springfield, MA). After exposing the fiber samples to UV radiation, SU-8 developer was used to remove the fibers that were not crosslinked. After rinsing the sample with developer solution, the sample was dried with nitrogen gas to remove any remaining developer solution. The patterned samples were inspected with the optical microscope and then transferred to clean sample vials and capped.

Instrumentation

All electron microscopy images of the electrospun fibers were obtained using a Hitachi S-4300 scanning electron microscope. Each SU-8 2100 sample was

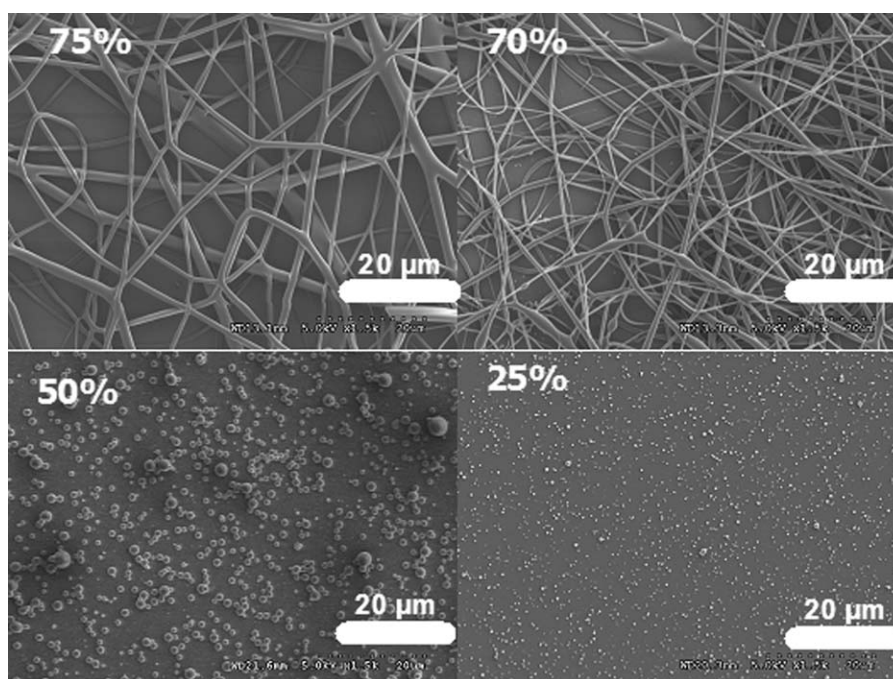


Figure 2 SEM images of the initial solutions of 75, 70, 50, and 25% SU-8 2100. Each sample was prepared at the same distance (10 cm), voltage (9 kV), and flow rate (0.02 mL/min).

sputter coated with gold prior to obtaining the images, while the pyrolyzed fiber samples were not coated to obtain images. The viscosity measurements were measured at room temperature using an Anton-Paar MCR300 rheometer with a concentric cylinder. A steady shear rate program was used to determine the viscosity, which was calculated over the linear range from 1 to 100 s^{-1} . Raman microscopy was performed on samples both before and after pyrolysis. Raman

experiments were performed using a Horiba Jobin Yvon HR800 Raman microscope with a 50 \times objective at a wavelength of 632 nm. To analyze the O/C atomic ratios, a Kratos Axis Ultra XPS was used with a monochromated Al X-ray gun and the ratios were determined taking the instrumental sensitivity into account. Samples were transferred directly from the quartz tube furnace to the XPS chamber and pumped overnight to $\sim 10^{-7}$ Torr before analysis. After the

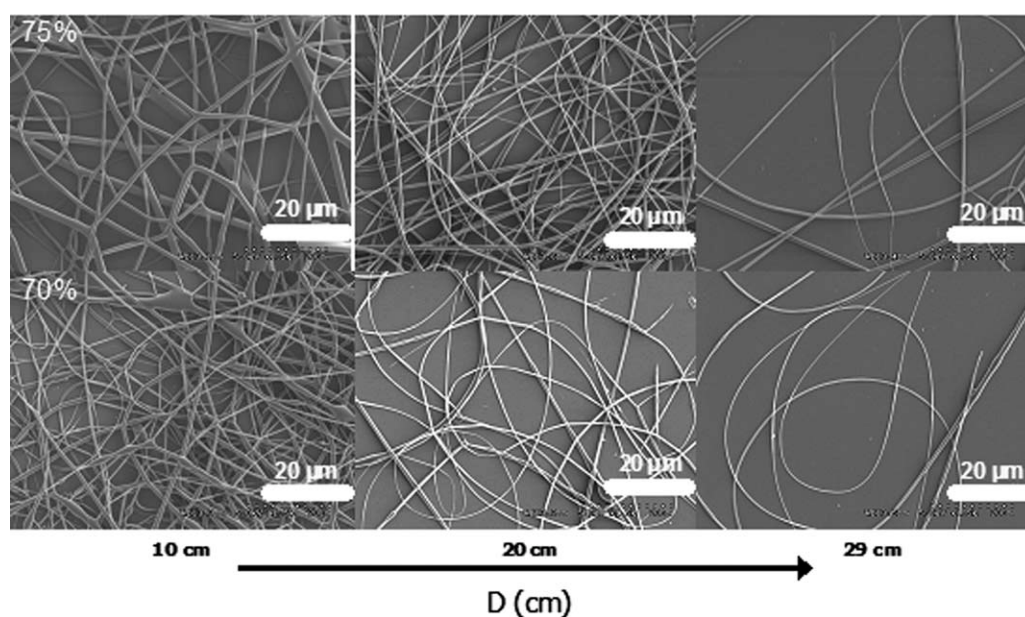


Figure 3 SEM images of the effect of distance on the electrospun SU-8 2100 fibers, where A is the 75% dilution and B is the 70% dilution. All samples were spun at 10 kV and a flow rate of 0.02 mL/min.

TABLE I
Effect of Distance on the Size of Electrospun SU-8 Fibers

% v/v SU-8	Distance (cm)	Average fiber size
75	10	$1.08 \pm 0.48 \mu\text{m}$
	15	$880 \pm 480 \text{ nm}$
	29	$830 \pm 350 \text{ nm}$
70	10	$770 \pm 390 \text{ nm}$
	15	$680 \pm 320 \text{ nm}$
	29	$530 \pm 170 \text{ nm}$

The voltage was held constant at 10 kV and the flow rate was kept constant at 0.02 mL/min.

initial analysis, the samples were exposed to air for 5 days and then the O/C ratios were again tested to determine the amount of oxidation that occurs with prolonged exposure to air.

RESULTS AND DISCUSSION

Effect of concentration and viscosity

Several different concentrations of SU-8 2100 were used to determine the concentrations at which electrospinning successfully resulted in fibers. The initial concentrations chosen were 100, 75, 50, 25, and 0% (v/v) SU-8 2100 in cyclopentanone. Viscosity is known to play a major role in the "spinnability" of a material and was also measured for each of the SU-8 solutions. Figure 1 shows the viscosity values obtained for the solutions that were examined. The viscosity measurements revealed the rheological differences between the various concentrations. The 75% and 70% SU-8 2100 solutions with viscosities of 1.17 Pa·s and 0.44 Pa·s, respectively, produced fibers;

the 50% and 25% SU-8 2100 concentrations with viscosities of 0.038 Pa·s and 0.0043 Pa·s, respectively produced beads. Both 100% and 0% SU-8 (pure cyclopentanone) concentrations resulted in no fibers or beads on the collector. Figure 2 shows SEM images of the resultant fibers and beads. For the remainder of experiments described, the concentrations of 75% and 70% SU-8 2100 were used to determine the optimal parameters for fibers and the 25% solution was used for the study of bead production because the beads were smaller and with a more uniform size distribution using the 25% solution compared to the 50% solution.

Effect of distance on fiber production

The optimal distance between the syringe tip and the collector for electrospinning SU-8 2100 was determined by using both the 75% and 70% SU-8 2100. The distances attempted were 10, 15, and 29 cm, while the flow rate and voltage were held constant at 0.02 mL/min and 10 kV, respectively. Figure 3 shows the SEM images of fibers resulting in the various distances for the 75% and 70% solutions. Using these parameters, Table I shows the average fiber diameters obtained for both the 75% and 70% concentrations. The fiber size obtained for the 70% SU-8 solution was smaller than the 75% SU-8 solution at the equivalent distances for the same electrospinning parameters.

Effect of voltage on fiber production

To test the effect of voltage on both solutions, the distance was set to 10 cm and the flow rate was

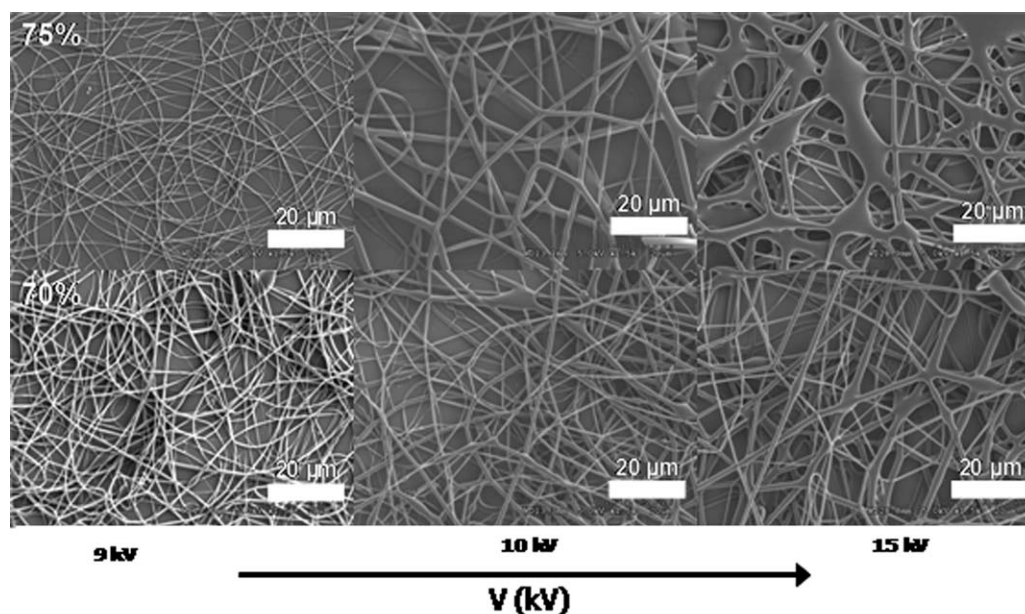


Figure 4 SEM images of the effect of voltage on SU-8 dilutions of 75% (A) and 70% (B). The distance was held constant at 10 cm and the flow rate was set to 0.02 mL/min.

TABLE II
Effect of Voltage on Electrospinning SU-8

% v/v SU-8	Voltage (kV)	Average fiber size
75	9	301 ± 30 nm
	10	1.08 ± 0.48 μm
	15	1.18 ± 0.83 μm
70	9	489 ± 140 nm
	10	770 ± 390 nm
	15	1.04 ± 0.51 μm

The distance was held at 10 cm and the flow rate was kept constant at 0.02 mL/min ($n = 15$).

kept constant at 0.02 mL/min. Figure 4 shows the SEM images obtained for both the 75% and 70% solutions at the several different voltages. The voltage that provided fibers with the smallest diameter for both dilutions was 9 kV. For both 75% and 70% concentrations, the fibers decreased in average diameter. The average diameters measured for both the 75% and 70% concentrations are shown in Table II. For the 70% solution, voltages below 9 kV (i.e., from 1 to 8 kV) were tested and did not provide any smaller diameter fibers but actually the fiber size increased slightly. At 5 kV, the 70% electrospun fibers were measured to be 830 nm ± 340 nm compared to 489 nm ± 138 nm for 9 kV. For the 75% SU-8 dilution, the average fiber diameters were measured and displayed an even larger relative decrease in size when electrospun at 9 kV. The average fiber diameter decreased from 1.08 μm (10 kV) to 301 nm (9 kV). Lower voltages were also tested for the 75% concentration. At a voltage of 5 kV, the average fiber diameter was 556 nm ± 305 nm which is a slight increase in fiber diameter when compared to the results for a voltage of 9 kV. 9 kV was shown to be the optimal voltage for both concentrations under the electrospinning parameters investigated.

Effect of flow rate on fiber production

The effect of SU-8 flow rate was also studied. For this study, only the 75% SU-8 concentration was tested since this concentration provides the smallest average fiber diameter. The voltage was held constant at 9 kV and the distance was set to 10 cm. The flow rates tested were 0, 0.005, 0.01, 0.02, 0.05, 0.1, and 0.2 mL/min. Figure 5 shows the effect of the flow rate on the fiber structure and size. The fiber structure and size was found to vary at flow rates higher than 0.02 mL/min. As is shown in Figure 5, using a flow rate of zero did not yield uniform fibers but broken fibers instead. Table III summarizes the average fiber diameters obtained for the flow rates tested. At the high flow rate of 0.2 mL/min, fibers were found present but the fiber diameter increased to 635 nm ± 379 nm. By comparing the size of the fibers at these flow rates, it can be determined that the flow rates between 0.005 to 0.02 mL/min yielded comparable fiber sizes.

Pyrolysis of electrospun SU-8 fibers and beads

Pyrolysis of electrospun SU-8 fibers is a simple way to generate carbon fibers. To convert the SU-8 nanofibers to carbon, the samples were placed in a quartz tube furnace under a forming gas (95% N₂ and 5% H₂) atmosphere. The samples were then heated at a rate of 1°C/min to 800°C and held at this temperature for a minimum of 5 h. Figure 6 shows the pyrolyzed fibers produced from both the 75% and 70% SU-8 2100 solutions. The fiber diameter decreased after pyrolysis but still maintained the same fiber structure that existed prior to heating. Also, Figure 7 shows the pyrolysis of 25% SU-8 to yield carbon beads. The unpyrolyzed beads had diameters of 420 ± 270 nm and 320 ± 140 nm after pyrolysis. It is also interesting to point out that to create the carbon

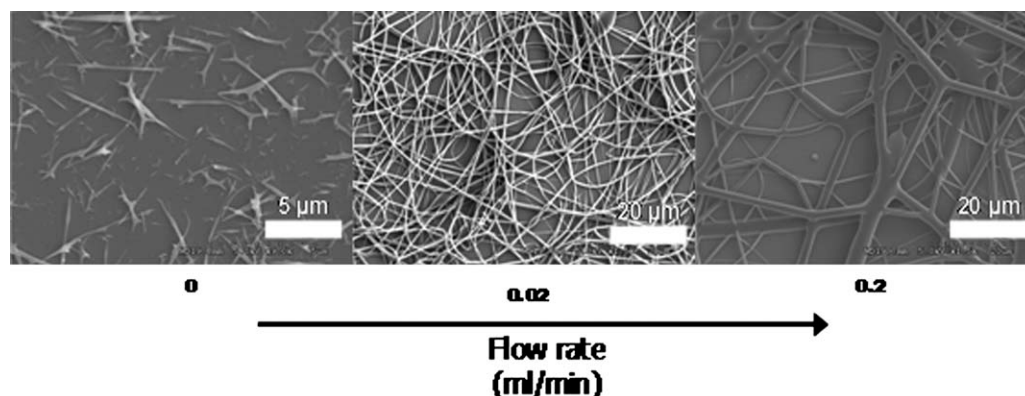


Figure 5 The effect of flow rate of electrospun SU-8 fibers. The distance and voltage was set at 10 cm and 9 kV, respectively.

TABLE III
The Effect of Flow Rate on Electrospinning SU-8

% v/v SU-8	Flow rate (mL/min)	Average fiber size (nm)
75	0.005	487 ± 220
	0.01	352 ± 180
	0.02	414 ± 150
	0.05	508 ± 430
	0.1	747 ± 1100
	0.2	635 ± 380

The voltage was kept constant at 9 kV and the distance was held at 10 cm ($n = 15$).

fibers or beads, the electrospun SU-8 material needs to be exposed to UV for at least 3 min to crosslink. If this step is not taken before pyrolysis, the fiber or bead structure is not maintained when converted to carbon. Instead, individual fibers or beads appeared to combine.

Patterning of electrospun SU-8 fibers

An advantage to electrospinning SU-8 photoresist is that electrospun fiber patterns can be generated. Figure 8 shows an SEM image of a pattern generated by exposing portions of the fiber mat to UV light after electrospinning. This process differs from what has typically been described in electrospinning as patterning. In electrospinning, the fibers are typically patterned by using different collectors. By using different collectors, the orientation or alignment of the

fibers can be changed. It has been shown that by altering the shape and structure of the collector allows for the fibers to produce several different patterns.^{18–20} Though these patterns generate aligned or oriented fibers, most of them do not provide a method to pattern the nonwoven fibers into several different patterns. The advantage of being able to pattern fibers through UV radiation is that UV photolithography can be used to easily generate any fiber pattern. The ease of creating a patterned mat of SU-8 fibers leads to many application possibilities. Similar patterning of electrospun nanobeads is also possible.

Fiber characterization

To characterize the fibers, the Raman spectra of the electrospun SU-8 fibers were acquired. The Raman spectra of the electrospun fibers were obtained after pyrolysis for fibers produced with 75% and 70% SU-8 to assess the sp^2 characteristic carbon bands at $\sim 1360\text{ cm}^{-1}$ (“D” band) and $\sim 1600\text{ cm}^{-1}$ (“G” band). Figure 9 shows the Raman spectra of the 75% and 70% SU-8 electrospun fibers after pyrolysis. For the 75% case, a peak at $\sim 950\text{ cm}^{-1}$ is the second order peak of the silicon substrate under the fiber mat (i.e. it is an impurity peak).¹⁰

By using the D and G bands, the disorder of the carbon sp^2 matrix can be determined. The ratio, $R = I_D/I_G$, of the integrated peak areas was determined using a Gaussian-Lorentz fit. The ratios were determined by taking the average of the peak area for

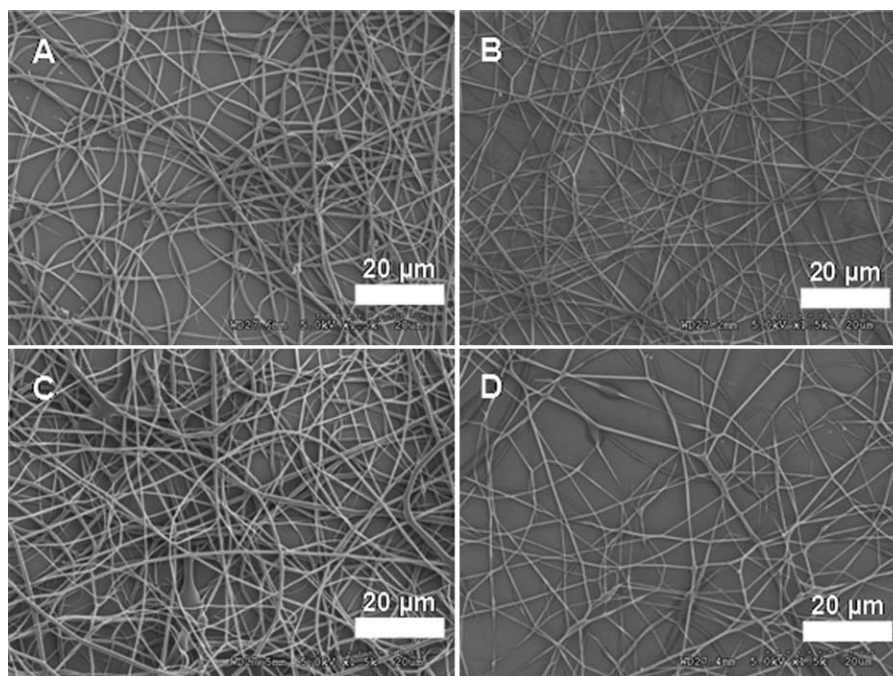


Figure 6 SEM images of the electrospun SU-8 fibers for the (A) unpyrolyzed 75% SU-8, (B) pyrolyzed 75% SU-8, (C) unpyrolyzed 70% SU-8, and (D) pyrolyzed 70% SU-8.

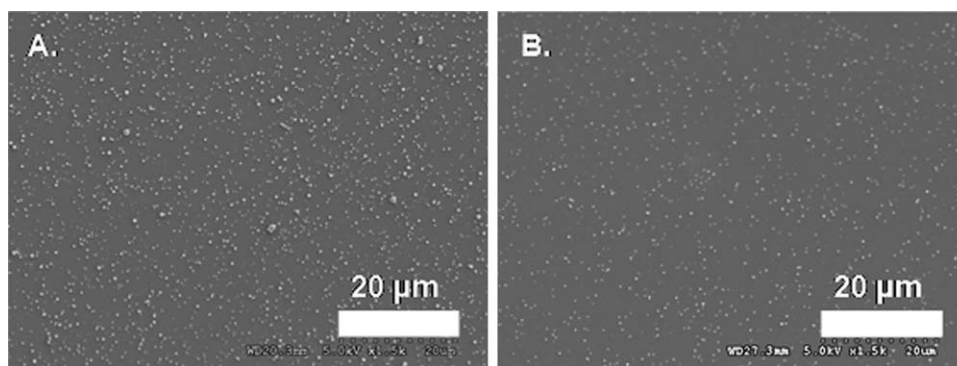


Figure 7 SEM images of 25% SU-8 2100 unpyrolyzed (A) and pyrolyzed (B) beads.

three random spots on each of the pyrolyzed samples. The ratio determined from the peak areas for the pyrolyzed 70% SU-8 pyrolyzed electrospun fibers was 1.20 ± 0.10 and the ratio determined for the 75% SU-8 pyrolyzed fibers was 1.14 ± 0.14 . On the basis of these ratios and the wavelength-corrected Tuinstra-Koenig relationship,²² a disordered nanocrystalline carbon network with crystallite sizes averaging $L_c = 7.1$ nm was produced under these conditions.²³ The similarity of the *D* to *G* ratio for the 70 and 75% SU-8 pyrolyzed fibers suggests that both concentrations result in glassy carbon fibers with similar molecular structure after pyrolysis.

CONCLUSION

In summary, this work describes an optimized process to generate electrospun fibers and beads from an SU-8 2100 negative photoresist. The electrospun SU-8 fibers generated had diameters ranging from 300 nm to 1 μm and are dependent upon the set of

parameters used. These fibers were also shown to be easily patterned by UV and then converted to carbon fibers via pyrolysis. It was also shown that the fiber or bead structure is maintained after pyrolysis. By utilizing the advantage of patterning the fibers after electrospinning, many applications ranging from microfluidics, sensors to micro/nanoelectronic can potentially be achieved.

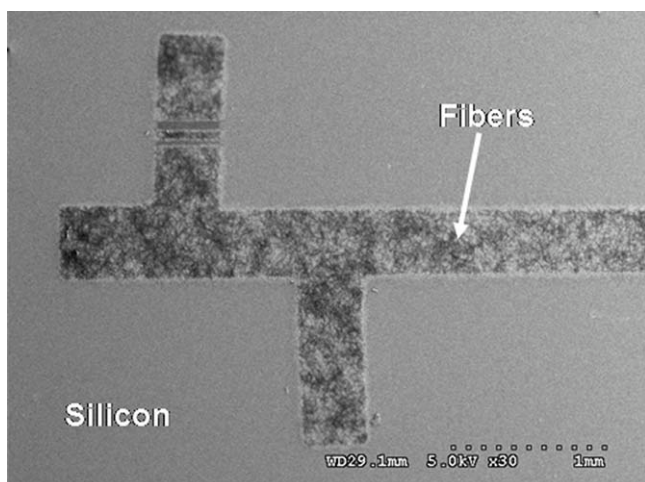


Figure 8 SEM image of UV patterned electrospun SU-8 fibers.

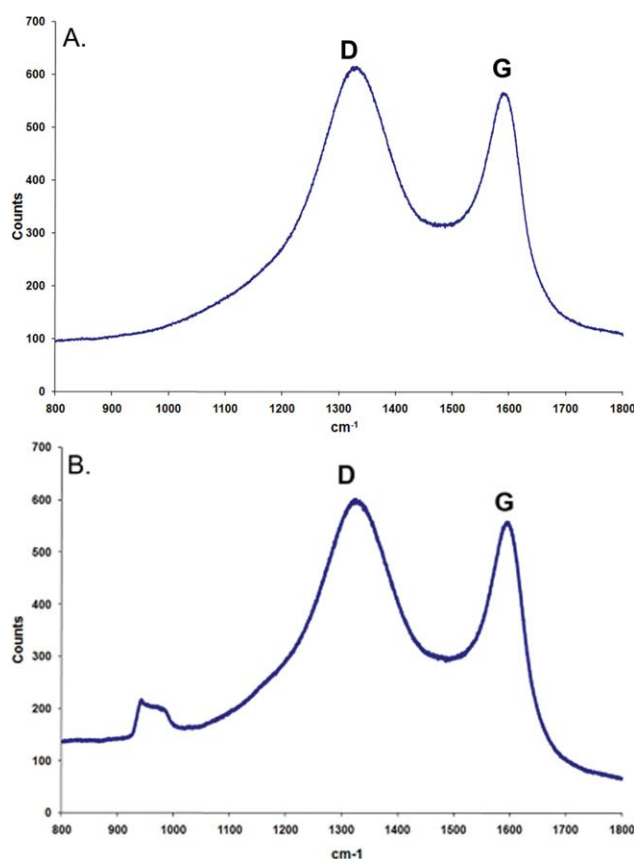


Figure 9 Raman microscopy spectra of the pyrolyzed electrospun SU-8 fibers from concentrations of 70% (A) and 75% (B). [Color figure can be viewed in the online issue, which is available at www.interscience.wiley.com.]

References

1. Renneker, D. H.; Yarin, A. L. *Polymer* 2008, 49, 2387.
2. Boudriot, U.; Dersch, R.; Greiner, A.; Wendorff, J. H. *Artif Org* 2006, 30, 785.
3. Aussawasathien, D.; Dong, J.-H.; Dai, L. *Synth Met* 2005, 154, 37.
4. Shim, W. G.; Kim, C.; Lee, J. W.; Yun, J. J.; Jeong, Y. I.; Moon, Y.; Yang, K. S. *J Appl Polym Sci* 2006, 102, 2454.
5. Luoh, R.; Hahn, H. T. *Compos Sci Technol* 2006, 66, 2436.
6. Ding, B.; Kim, J.; Miyazaki, Y.; Shiratori, S. *Sens Actuators B* 2004, 101, 373.
7. Moran-Mirabal, J. M.; Slinker, J. D.; Defranco, J. A.; Verbridge, S. S.; Ilic, R.; Flores-Torres, S.; Abruña, H.; Malliaras, G. G.; Craighead, H. G. *Nano Lett* 2007, 7, 458.
8. Pinto, N. J.; González, R.; Johnson, A. T., Jr.; Macdiarmid, A. G. *Appl Phys Lett* 2006, 89, 033505.
9. Ramakrishna, S.; Fujihara, K.; Teo, W.; Lim, T.-C.; Ma, Z. *An Introduction to Electrospinning and Nanofibers*; World Scientific Publishing Co. Pte. Ltd.: Toh Tuck Link, Singapore, 2005.
10. Gu, S. Y.; Ren, J.; Wu, Q. L. *Synth Met* 2005, 155, 157.
11. Wang, Y.; Serrano, S.; Santiago-Aviles, J. J. *J Mater Sci Lett* 2002, 21, 1055.
12. Zussman, E.; Chen, X.; Ding, W.; Calabri, L.; Dikin, D. A.; Quintana, J.; Ruoff, R. S. *Carbon* 2005, 43, 2175.
13. Park, S. H.; Kim, C.; Choi, Y. O.; Yang, K. S. *Carbon* 2003, 41, 2653.
14. Chung, G. S.; Jo, S. M.; Kim, B. C. *J Appl Polym Sci* 2005, 97, 165.
15. Rutledge, S. L.; Shaw, H. C.; Benavides, J. B.; Yowell, L. L.; Chen, Q.; Jacobs, B. W.; Song, S. P.; Ayres, V. M. *Diamond Relat Mater* 2006, 15, 1070.
16. Zheng, G.-B.; Kouda, K.; Sano, H.; Uchiyama, Y.; Shib, Y. F.; Quan, H. J. *Carbon* 2004, 42, 635.
17. Endo, M.; Kima, Y. A.; Takedaa, T.; Honga, S. H.; Matusita, T.; Hayashia, T.; Dresselhaus, M. S. *Carbon* 2001, 39, 2003.
18. Igarashi, S.; Tanaka, J.; Kobayashi, H. *J Nanosci Nanotechnol* 2007, 7, 814.
19. Li, D.; Ouyang, G.; Mccann, J. T.; Xia, Y. *Nano Lett* 2005, 5, 913.
20. Zhang, D.; Chang, J. *Adv Mater* 2007, 19, 3664.
21. Lee, K. Y.; Labianca, N.; Rishton, S. A.; Zolgharnain, S.; Gelorme, J. D.; Shaw, J.; Chang, T. H. P. *J Vac Sci Technol B* 1995, 13, 3012.
22. Matthews, M. J.; Pimenta, M. A.; Dresselhaus, M. S.; Endo, M. *Phys Rev B* 1999, 59, R6585.
23. Ferrari, A. C.; Robertson, J. *Phys Rev B* 2000, 61, 14095.